Effect of harvesting month and proximity to fish farm sea cages on the lipid profile of cultivated *Saccharina latissima*

João P. Monteiro [a,b,*], Tânia Melo [a,b], Jorunn Skjermo [c], Silje Forbord [c], Ole J. Broch [c], Pedro Domingues [a], Ricardo Calado [d], M. Rosário Domingues [a,b]

[a] *CESAM – Centre for Environmental and Marine Studies, Department of Chemistry, University of Aveiro, Santiago University Campus, 3810-193 Aveiro, Portugal*
[b] *Mass Spectrometry Centre, LAQV REQUIMTE, Department of Chemistry, University of Aveiro, Santiago University Campus, 3810-193 Aveiro, Portugal*
[c] *SINTEF Ocean, N-7465 Trondheim, Norway*
[d] *CESAM – Centre for Environmental and Marine Studies, Department of Biology, University of Aveiro, Santiago University Campus, 3810-193 Aveiro, Portugal*

A B S T R A C T

Macroalgae aquaculture is thriving, and kelps such as *Saccharina latissima*, are now farmed over different production sites across Europe. Macroalgae production in integrated multi-trophic aquaculture setups is gaining relevance due to increased biomass yield and bioremediation potential. Nevertheless, there is a substantiated need to understand how this type of production shapes biomass composition. The present study evaluated the influence of time of harvesting and proximity to nutrient source (fish farm sea cages) on the elemental and biochemical composition of *S. latissima,* with special emphasis on its lipid content. Overall, the differences recorded for elemental, biochemical and lipid composition of *S. latissima* occurred consistently with harvesting period rather than with the distance to fish farm sea cages, evidencing that farming kelp in integrated multi-trophic aquaculture setups does not compromise nutritional quality while promoting increased biomass yield. Elemental and biochemical composition differed between kelp biomass harvested in April and those harvested in May and June, with lower C, H and carbohydrates, and higher ash contents in the later. Fatty acid profile analysis revealed an increase in monounsaturated fatty acids along the harvesting period, as well as a decrease in *n*-3 fatty acids with a concomitant increase of the *n*-6/*n*-3 ratio from April to May. Statistical analysis of the polar lipidome identified by liquid chromatography-mass spectrometry revealed differences in specific lipid signatures, displaying a perfect discrimination between harvesting periods. The discrimination between samples from reference and integrated multi-trophic aquaculture sites was only observed for kelp biomass harvested in June. Contributing particularly to these differences are betaine lipids, more abundant in the two later time points, and some lysolipid species, especially abundant in June. These findings will allow a more integrated look at macroalgae production under integrated multi-trophic aquaculture framework, thus promoting the systematization of farming practices that may enhance yield with biochemical quality to match the increasing demands by the food industry and sustainable biorefinary pipeline.

1. Introduction

Increased demographical pressure has led to the search for innovative nutritional/industrial expedients, and for the exploitation of otherwise neglected living resources. Macroalgae are established nutritional resources as well as recognized sources of bioactive compounds [1–3], with great potential for decisively contributing to a future bio-based society. Given this great potential and increasing significance as

viable resources for a number of industries, the implementation of macroalgae aquaculture production sites in the open sea constitutes a seductive approach. This approach may contribute to the growing demands from the food market and represent a viable way of supplying an industrial biorefinery pipeline, without a demand for fresh water or fertile land.

By 2016, the global production of farmed seaweed reached 30 million and approximately 27% of this production was kelp [4], a group

of large brown seaweeds of the Laminariales order.Of these, *Saccharina latissima* (Linnaeus) C.E.Lane, C.Mayes, Druehl & G.W.Saundersis one of the most commonly cultivated species, given its relatively fast growth and substantial biomass yield, along with its wide geographical distribution [5–7]. Moreover, this species has high nutritional value with a very interesting content in essential minerals, sugars and proteins, and, also contain many other valuable compounds, namely phenolics, fucoidan, fucoxanthin, and alginates with several industrial applications [8–12]. Therefore, many *S. latissima* cultivation sites were established in the European North Atlantic, from Galicia (Spain) to the Scandinavian countries [13]. In addition, recent studies acknowledged the nutritional interest of *S. latissima* namely regarding its lipid content, reporting the presence of a considerable percentage of *n*-3 polyunsaturated fatty acids (PUFA) [14–18]. Moreover, the polar lipidome profile of this kelp in terms of its composition in glycolipids, phospholipids and betaines lipids was also previously profiled in detail [15,18]. These lipidomics studies deeply identified and quantified the lipid composition of this kelp, in terms of lipid classes and species, some of them already ascribed bioactive properties, and others representing important carriers of *n*-3 PUFA. A remarkable plasticity and flexibility in terms of lipid composition was also uncovered, according to the geographic origin at a European scale [18].

Macroalgae are known to adapt to shifting environmental conditions by changing their nutrient uptake efficiency, photosynthetic activity, and secondary metabolism [19–21]. Both abiotic and biotic factors were reported to strongly influence the biochemical composition of macroalgae [22]. The different factors known to influence macroalgae chemical composition include light, temperature, salinity, CO_2 concentration, local nutrient availability, contaminants and biotic interactions, among others [22–29]. In the case of *S. latissima,* it was already reported that differences in growth location, impact morphology and biomass yield and composition [7,8,11,18]. Moreover, some of these environmental factors can be susceptible to change according to production system, sites and harvesting period.

The time of harvesting consistently documented as determining biochemical composition, thus likely influencing the content of compounds that may represent an added-value to macroalgae biomass. In fact, it was already shown that carbohydrates of S. latissima significantly vary with season [30–33], as well as protein [31], and ash [31,32] contents. Regarding lipids, it was reported higher lipid content in the winter months, and a tendency to increased contents in total FA [14,16], whereas a tendency for decreased levels of unsaturation in the warmer summer months was also described [16].

Differences between wild and cultivated biomass in terms of lipid total content were already reported for *S. latissima* farmed under different conditions [16]. It was described that samples originated from nutrient-enriched waters from a nearby fish farm, under an integrated multi-tropic aquaculture system (IMTA), contained a remarkably higher fatty acid (FA) content (60% more) than wild conspecifics, with farmed kelps featuring more eicosapentaenoic acid (FA 20:5) and a significantly lower *n*-6/*n*-3 ratio [16]. However, another study failed to demonstrate significant differences in lipid and FA content between *S. latissima* cultivated within or outside IMTA [14], thus revealing the need for further studies on this topic.

In the present study we performed a thorough analysis of *S. latissima* elemental, biochemical and polar lipidome composition in order evaluate the relevance of time of harvesting and the farming of this species under an IMTA framework. We hypothesize that harvesting time and production setup type will impact biomass yield and composition, with physiological and biological drivers potentially contributing to putatively observed differences. A state-of-the-art GC–MS and high-resolution LC-MS-based lipidomic approach was used to compare kelp biomass and unravel potential differences at molecular level promoted by time of harvesting and IMTA production. This work aims to contribute to an optimized culture of kelps, adding value to produced biomass and increasing the revenues for the macroalgae industry.
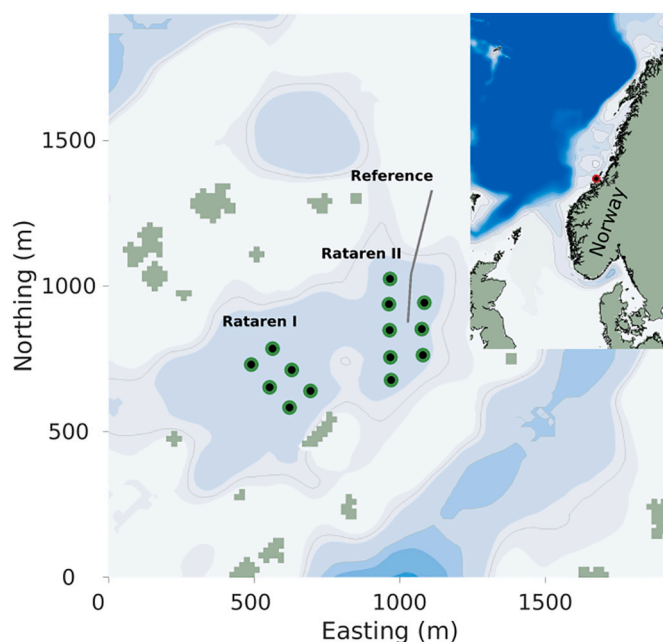

Fig. 1. Layout of the fish farm at Rataren and the IMTA setup. The green/black circles indicate the positions of the fish cages, organized into a western (Rataren I) and an eastern (Rataren II) array. The heavy, gray lines indicate the layout of the *S. latissima* long lines, with the position of the reference station at the northeasternmost end. The thin, gray curves are 25, 50, and 100 m isobaths. The inset map shows the position of the site at 63°78′N, 08°53′E. (For interpretation of the references to color in this figure legend, the reader is referred to the web version of this article.)

2. Materials and methods

2.1. Field trial

Sporophytes of *S. latissima* with mature sori were collected near the study site in December 2017 and shipped to the laboratory for production of seed lines. Seedlings were produced by seeding spores on 1.2-mm diameter twine coiled around PVC spools [34]. The spools were incubated for 6 weeks in nutrient-rich deep water and when the seedling reached a size of ~0.5 mm in length the twines were machine-transferred to 16 mm ropes. The 5 m long ropes were then deployed vertically at sea at the fish farm of Rataren outside the island of Frøya in Central Norway (63–78′N, 08–53′E; Fig. 1) on February 16th 2018 approximately 10 m apart on 22 mm thick longlines 1 m below the sea surface. The longlines were placed between salmon farming sea cages (IMTA) as well as in a reference location (REF), placed at 150 to 300 m from the corner of the outmost sea cage (Fig. 1). This area has a mild maritime climate with the coldest season from January to March and the driest season in May to June [12], and the sea temperature typically varies between 4.5 °C in mid-March to 10.2 °C at the beginning of June. Average monthly temperatures never reached more than 9.8 °C [35].

2.2. Numerical modelling

The coupled physical-biological model system SINMOD was used to simulate the concentrations and dispersal of ammonium from the fish farm. SINMOD has previously been used to simulate the ammonium dispersal from finfish farms in Norway [36]. The hydrodynamic calculations in SINMOD are based on the primitive Navier-Stokes equations solved by a finite difference scheme on an Arakawa C-grid [37].

SINMOD has previously been established for the region around the fish farm at Rataren, and has been shown to realistically reproduce the currents in the region [38,39]. The model domain covers a region of
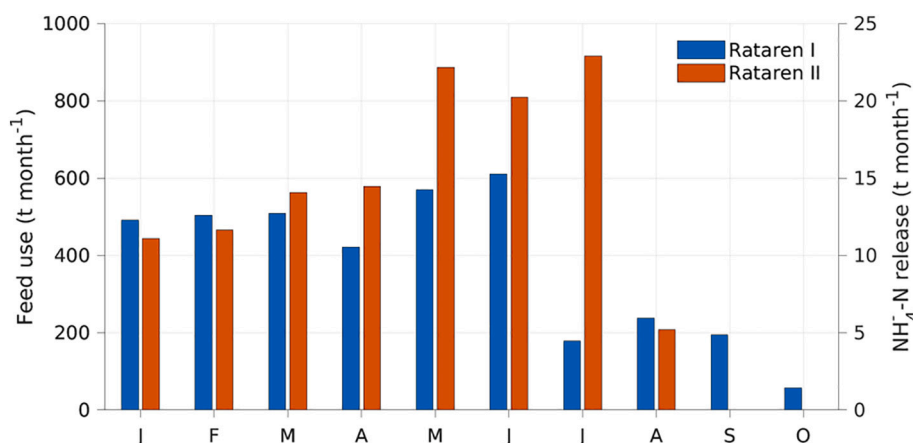
Fig. 2. The feed used at the two fish cage arrays (I and II) at Rataren (left vertical axis) and the corresponding release of ammonium used in the numerical simulations (right vertical axis). See Fig. 1 for the layout of the farm.

approx. 22 by 18 km in a horizontal resolution of 32 m, and uses depth layers of 0.5–2 m thickness from the surface down to 25 m depth and further layers of 5–25 m thickness from 25 to 250 m depth. Detailed information about nesting, atmospheric, and freshwater forcing of this model setup has been described before [38,39]. For the present application of SINMOD, the fish farm structures may affect the water currents, e.g. by reducing the water current speed just "downstream" of the farm [39]. The release of ammonium from the farm was calculated from the feed use as described previously [36]· (Fig. 2), and was assumed to be released homogeneously from each cage (Fig. 1) from 3 to 20 m depth, constantly over each month. The total feed used for each of the cage arrays (Rataren I and II) were distributed equally over the corresponding fish cages.

2.3. Sampling and evaluation of biomass development

Registrations were performed in April 23rd, May 29th and June 13th 2018 from 4 to 16 ropes per cultivation condition. At each sampling time, kelp biomass (kg m^{-1}) from each rope was weighted and excess water was minimized by letting it run off for 30 s before weighing the kelp biomass to the nearest 0.1 kg. The biomass weight was determined either by weighting the whole rope or by harvesting subsamples. The sporophytes from 50 cm of the upper 1–1.5 m part of the ropes were harvested, weighted, counted and the maximum length and width measured for 20 haphazardly selected sporophytes. Further, 20 sporophytes from each batch, each consisting of the frond, stipe and holdfast, were collected for analysis of chemical composition. Sporophytes were carefully shaken to minimize excess water and placed in individual plastic zip lock bags without removing epibionts. The samples were transported onshore in coolers and stored at −20 °C after arriving to the laboratory. Before chemical analysis the samples were frozen at −80 °C before freeze dried (Heterosicc CD 13-2) at −40 °C for 48 h.

2.4. Biochemical and elemental composition

Ash was determined by a two-step procedure. Biomass was first pre-incinerated in crucibles and then transferred into a muffle furnace, where they were kept at 575 °C for 6 h. After cooling to room temperature, crucibles were weighed and the ash content determined.

The elemental composition of the biomass in terms of carbon (C), hydrogen (H), nitrogen (N) and sulphur (S) was analyzed using a Leco Truspec-Micro CHNS 630–200-200 elemental analyser (Leco Corporation, Geleen, The Netherlands), with a combustion furnace temperature of 1075 °C and afterburner temperature 850 °C. About 2 mg of biomass were burned in an oxygen/carrier gas mixture, in conditions guaranteeing full combustion and also the conversion of a few by-products into

water vapor, carbon dioxide and nitrogen for gas analysis. Carbon, hydrogen and sulphur were detected by infrared absorption, while nitrogen was determined by thermal conductivity. Protein content was estimated by the use of a nitrogen-to-protein conversion factor of 3.9, a factor determined based on measurement of total amino acids for locally cultivated *S. latissima* sporophytes [40]. Content in carbohydrates (and other compounds) was estimated by subtraction of the percentage of ash, lipids, and proteins in samples from 100%.

2.5. Lipid extraction

Total lipid extracts were obtained by standard methods used in our lab [15,18]. After a step of homogenization by grinding freeze-dried samples using a mortar and pestle, samples of 250 mg of macroalgae biomass were immersed in 2.5 mL of methanol and 1.25 mL of dichloromethane in glass centrifuge tubes, vortexed (2 min) and sonicated (1 min), and then incubated on ice for 2 h and 30 min in an orbital shaker. Afterwards, tubes were centrifuged at 626 x*g* for 10 min at room temperature and the organic phase, was collected. Two re-extraction steps were performed by adding each time 2 mL of methanol and 1 mL of dichloromethane, and the resulting supernatants were added the first organic phase obtained. A volume of 2.5 mL of ultrapure water were added to each tube, resolving a two-phase system. Samples were then again centrifuged at 626 x*g* for 10 min at room temperature, and the lower organic phase was collected into a new tube. These purified fractions were dried under a nitrogen stream and the final weights of the total lipid extract were determined by gravimetry. Finally, extracts were stored at −20 °C until further analysis.

2.6. Fatty acid analysis (gas chromatography–mass spectrometry)

Fatty acid content in total lipid extracts was studied by GC–MS after transmethylation [15,18]. Aliquots of 30 μg of lipid extracts were transferred to Pyrex glass tubes and then dried under nitrogen current. The resulting lipid film was resuspended in 1 mL of n-hexane containing a C19:0 internal standard (1 μg mL^{-1}, CAS number 1731-94-8, Merck, Darmstadt, Germany). A volume of 200 μL of a methanolic solution of potassium hydroxide (2 M) was added to each tube and the mixture was vortexed for 2 min. A volume of 2 mL of a saturated solution of sodium chloride was then added to the tubes, and the resulting mixture was centrifuged for 5 min at 626 x*g*, promoting phase separation. The upper phase, containing the fatty acid methyl esters (FAMEs) was then transferred into a microtube and dried under nitrogen current. FAMEs were resuspended in 50 μL *n*-hexane, and 2 μL of the resulting solution were injected for GC–MS analysis on an Agilent Technologies 6890 N Network Chromatograph (Agilent, Santa Clara, CA, USA) equipped with a DB-

FFAP column with 30 m length, an internal diameter of 0.32 mm and a film thickness of 0.25 μm (J&W Scientific, Folsom, CA, USA). The gas chromatographer was connected to an Agilent 5973 Network Mass Selective Detector (Agilent, Santa Clara, CA, USA) operating with an electron impact mode at 70 eV and scanning the mass range m/z 50–550 in a 1 s cycle in a full scan mode acquisition. Oven temperature was set to maintain initially a temperature of 80 °C for 3 min, a step followed by three consecutive linear increments to 160 °C at 25 °C minute^{-1}, to 210 °C at 2 °C minute^{-1}, and to 250 °C at 30 °C minute^{-1}. Temperature was finally set to be maintained at 250 °C for 10 min. Injector and detector temperatures were 220 and 280 °C, respectively. Helium was used as carrier gas, with a flow rate set at 1.3 mL min^{-1}. Fatty acid assignment was accomplished by comparing the retention times to those of the commercial FAME standards in the Supelco 37 Component FAME Mix (ref. 47885-U, Sigma-Aldrich, Darmstadt, Germany), and mass spectra obtained to those accessible in databases. Parameters such as the average chain length (ACL), double bond index (DBI), peroxidizability index (PI), content in monounsaturated fatty acids (MUFA), polyunsaturated fatty acids (PUFA), polyunsaturated fatty acids n-3 (PUFA n-3) and polyunsaturated fatty acids n-6 (PUFA n-6) were calculated as previously described.

2.7. Polar lipidome analysis (hydrophilic interaction liquid chromatography-mass spectrometry and tandem mass spectrometry)

Total lipid extracts were analyzed by hydrophilic interaction liquid chromatography on a high-performance liquid chromatography (HPLC) Ultimate 3000 Dionex (Thermo Fisher Scientific, Bremen, Germany), with an autosampler coupled online to a Q-Exactive hybrid quadrupole mass spectrometer (Thermo Fisher, Scientific, Bremen, Germany). The resolving solvent system consisted of two mobile phases: mobile phase A, containing water, acetonitrile and methanol (25%, 50%, 25%), with 2.5 mM ammonium acetate, and mobile phase B, containing acetonitrile and methanol (60%, 40%), with 2.5 mM ammonium acetate. Elution was set to start at 10% of mobile phase A, held isocratically for 2 min, followed by a linear increase to 90% of this phase within 13 min, after which this value was maintained for 2 min, and later returned to the initial settings within 28 min (8 min for the decrease to the initial 10% of phase A, and a re-equilibration period of 10 min prior to the next injection). For HILIC-LC-MS analysis, an aliquot of 10 μg of total lipid extract, 2 μL of phospholipid standards mix (dMPC – 0.01 μg, dMPE – 0.01 μg, LPC – 0.01 μg, dPPI – 0.04 μg, dMPG – 0.006 μg, dMPS – 0.02 μg, tMCL – 0.04 μg, SM(17:0/d18:1) – 0.01 μg, dMPA – 0.04 μg) and 88 μL of eluent (10% of mobile phase A and 90% of mobile phase B) were mixed and a volume of 10 μL of the mixture injected into the microbore Ascentis Si column (10 cm × 1 mm, 3 μm, Sigma-Aldrich), with a flow rate of 50 μL minutes^{-1} at 35 °C. Acquisition in the Orbitrap® mass spectrometer was performed in both positive (electrospray voltage 3.0 kV) and negative (electrospray voltage −2.7 kV) modes, with high resolution with 70,000 and AGC target of 2e^6. Capillary temperature was set at 250 °C, and the sheath gas flow was 15 U. For MS/MS determinations, a resolution of 17,500 and AGC target of 1e5 was used, and the cycles consisted of one full scan mass spectrum, and ten data-dependent MS/MS scans repeated continuously throughout the experiments, with the dynamic exclusion of 60 s and an intensity threshold of 1e4. Normalized collision energy™ (CE) were set to range between 20, 25 and 30 eV. Data acquisition was performed using the Xcalibur data system (V3.3, Thermo Fisher Scientific, USA) [41]. For analysis, phospholipid peak integration and assignments were performed using MZmine version 2.40.1 [42]. The process included filtering and smoothing, peak detection, peak processing, and assignment against an in-house database. For all assignments, only ions within 5 ppm of the lipid exact mass were considered possible matches. Assigned polar lipid species were further validated by manual analysis of the MS/MS data as detailed before [18]. MGMG, DGMG, MGDG, DGDG, DGTS, PC, LPC, PE and LPE classes, were detected and quantified in the positive ion mode,
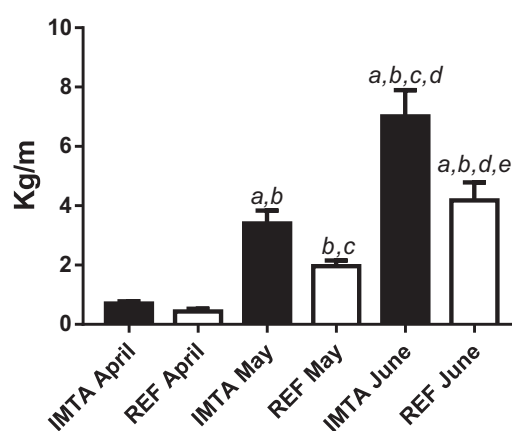

Fig. 3. Evaluation of biomass yield along the three harvesting months. Values depicted represent means ± STD ($n > 5$ for all groups). IMTA: integrated multitrophic aquaculture site; REF: reference site. Statistical significant differences ($q < 0.05$) are presented as follows: *a*: vs. IMTA April; *b*: vs. REF April; *c*: vs. IMTA May; *d*: vs. REF May; *e*: vs. IMTA June.

while SQDG, SQMG, LPG, PG, LPI and PI were analyzed in the negative ion mode. Relative lipid species quantitation was performed by exporting integrated peak areas values into a computer spreadsheet (Excel, Microsoft, Redmond, WA), and data normalization was accomplished by dividing the peak areas of the extracted ion chromatograms (XICs) of the polar lipid precursors of each polar lipid class by the peak area of the internal standard selected for that class.

2.8. Statistical analysis

Biomass yield, elemental and biochemical analysis graphs were produced using GraphPad Prism version 7.00 for Windows (GraphPad Software, La Jolla, California, USA). Multivariate and univariate analyses were performed using R version 3.5.1 [43] in Rstudio version 1.1.4 [44]. GC data were glog transformed and HPLC/MS data were glog transformed and autoscaled using the R package Metaboanalyst [45]. The statistical significance of differences among groups were assessed by performing the Kruskal-Wallis test, followed by Dunn's multiple comparison test, with Benjamini and Hochberg FDR correction (q values). Differences with q value <0.05 were considered statistically significant. All experimental data are shown as mean ± standard deviation (STD) (n = 5 replicate ropes per origin). Principal component analysis (PCA) was performed to visualize the general 2D clustering of replicates of the same origin in terms of FA and polar lipid species present, and was carried out with the R built-in function and ellipses were drawn using the R package ellipse [46], assuming a multivariate normal distribution and a level of 0.95. The Royston's Multivariate Normality Test [47] was performed using the R MVN package [48].Hierarchical clustering heatmaps were created using the R package pheatmap [49] using "Euclidean" as clustering distance, and "ward.D" as the clustering method. All graphics and boxplots were created using the R package ggplot2 [50]. Other R packages used for data management and graphics included plyr [51], dplyr [52], and tidyr [53].

3. Results

3.1. Evaluation of biomass production

Production in IMTA promoted a significantly higher biomass yield over the three harvesting periods with a final average weight of 7.0 ± 0.9 kg m^{-1} compared to 4.5 ± 0.8 kg m^{-1} at REF in June (Fig. 3).
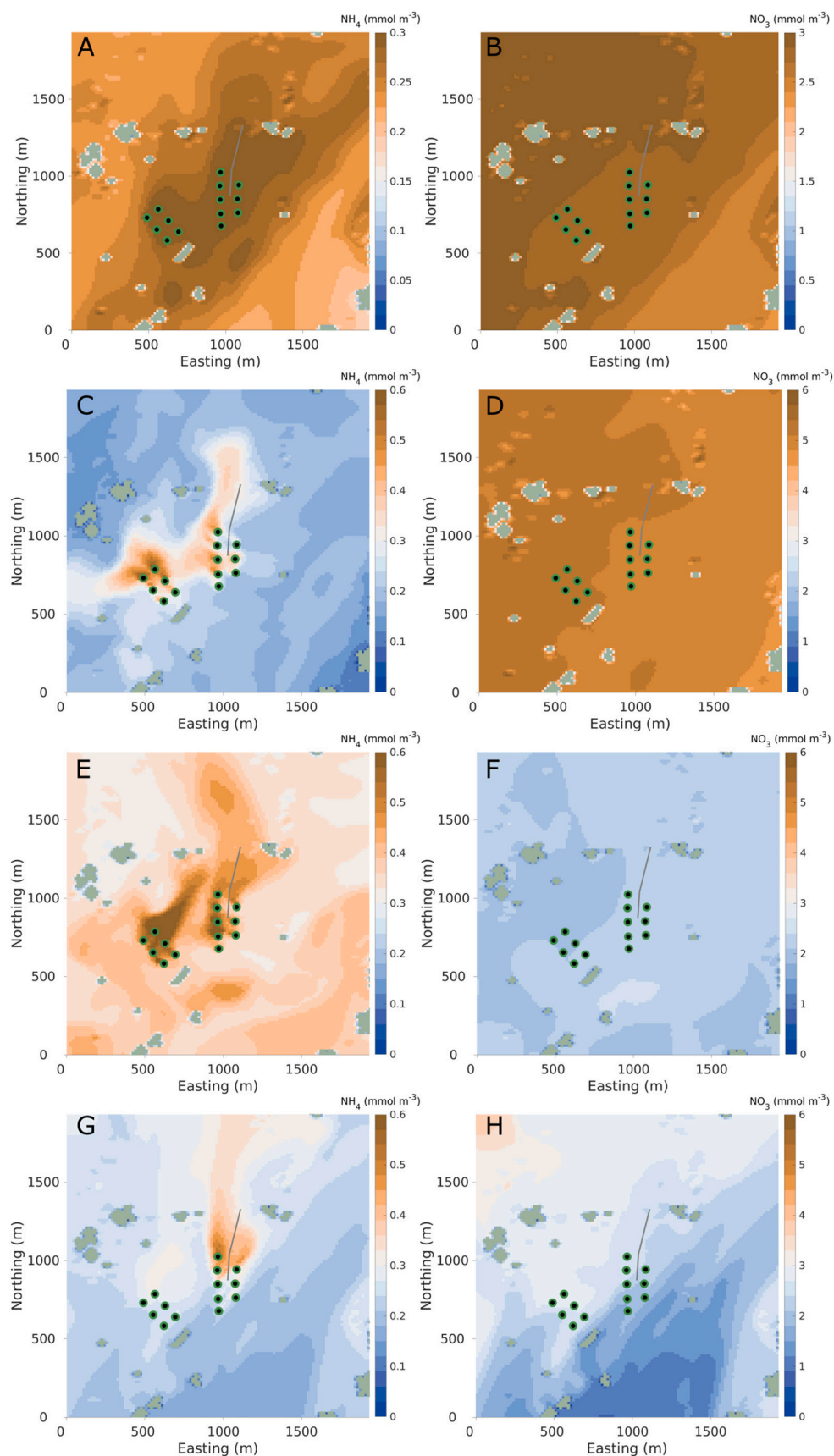
Fig. 4. Simulated, depth integrated (0–6 m) NH$_4^+$ and NO$_3^-$ concentrations. Panels A and B display time averaged (April–June) simulated NH$_4^+$ and NO$_3^-$ concentrations, respectively. Panels C – H are snap shots of simulated NH$_4^+$ and NO$_3^-$ concentrations on April 23 (C, D), May 29 (E, F), and June 13 (G, H).
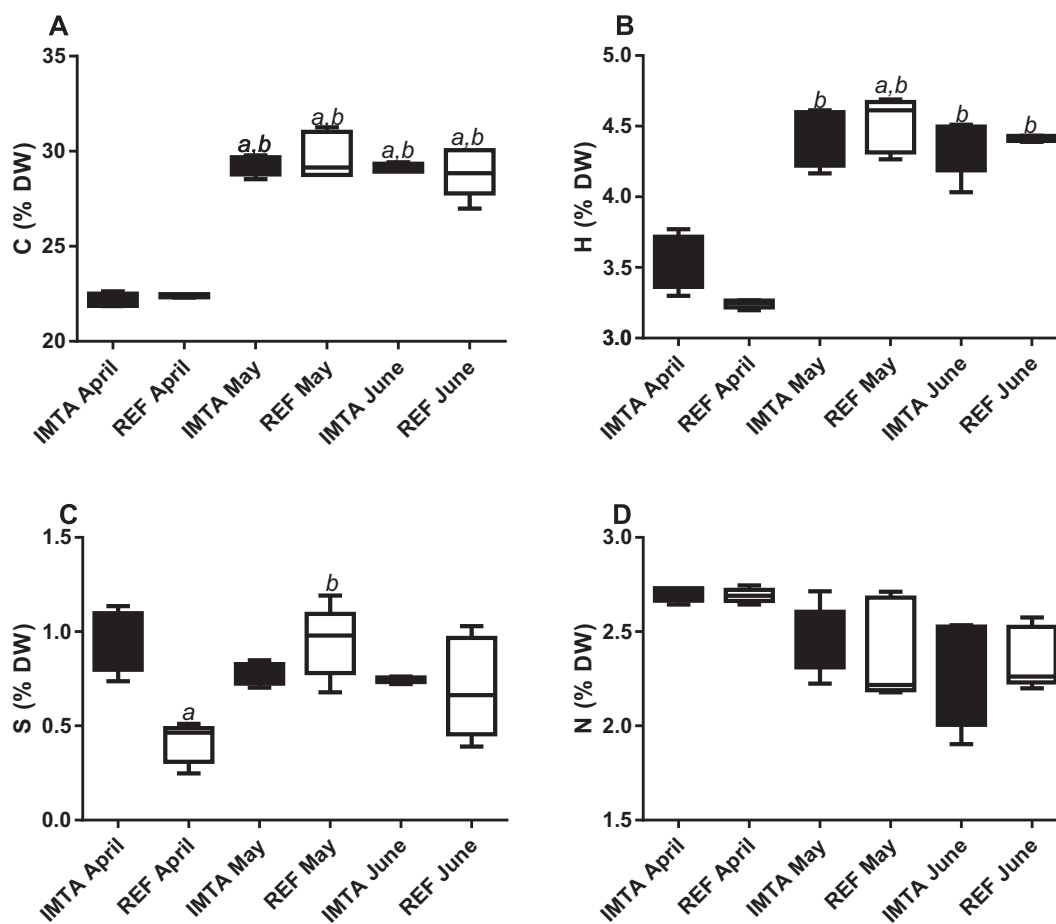
Fig. 5. Elemental analysis of *S. latissima* samples from different types (REF or IMTA), harvested in different months (April, May and June). Content in carbon (A), hydrogen (B), sulphur (C) and nitrogen (D) are presented as percentages of DW. IMTA: integrated multi-trophic aquaculture site; REF: reference site. Values depicted represent means ± STD for 5 replicates (ropes). Statistical significant differences ($q < 0.05$) are presented as follows: *a*: vs. IMTA April; *b*: vs. REF April.

3.2. Numerical modelling

The average (April 23 to June 13) depth integrated (0–6 m) simulated NH_4^+ concentrations were clearly higher in and around the fish farm than in the surrounding waters (Fig. 4 A, left). The kelp long lines were positioned based on current measurements from the fish farm. According to the simulation results, the IMTA long lines were positioned firmly within the ammonium "plume" from the farm, and there was a clear gradient in ammonium concentration, in particular form the northern most cages and in the northern-north eastern direction on the long lines (Fig. 4 A). The time averaged simulated NH_4^+ concentrations were almost an order of magnitude lower than the corresponding NO_3^- concentrations (Figs. 3 A, B). The simulated background NO_3^- concentrations decreased from 4.5 mmol NO_3^- m^{-3} in April to 2 mmol NO_3^- m^{-3} i May–June (Figs. 3 D, F, H). The snap shot from June (Fig. 4 H) indicates that the NO_3^- was heterogeneously distributed around the farm at this time, probably caused by episodal vertical mixing of more nutrient rich deeper water in part of the model domain. The farm site is tidally influenced [39], also seen from the snap shots (Figs.3 C, E and G) indicating that there are periodic "pulses" with relatively high NH_4^+ concentrations.

3.3. Elemental and biochemical analysis

The elemental analysis revealed some differences between groups (Fig. 5), namely between harvesting periods, and more obviously between April and the following months. Significant differences related with harvesting period were recorded for carbon, hydrogen and sulphur

content, suggesting a tendency for increased carbon and hydrogen content in latter harvesting periods (May and June) (Fig. 5). There also seems to be a tendency for lower N content at later harvesting periods. These differences are essentially inter-monthly, with the exception of sulphur content in April, where statistical difference was observed between reference and IMTA samples (Fig. 5C).

Regarding ash, protein, lipid and carbohydrate contents, statistically significant differences were observed exclusively between different harvesting times (Fig. 6). There was a trend for a decrease in ash content and an increase in the content in carbohydrates from April to June (Fig. 6A and D). Therefore, the increase in carbon, hydrogen and sulphur (in this case in May and June regarding April, only in samples from REF sites; Fig. 5), may happen in the form of organic compounds, namely sulphated carbohydrates, which increase with time (Fig. 6D). Lipid content (ranging from 1.30 ± 0.06% in IMTA samples from April to 0.83 ± 0.06% in REF samples from June) was generally higher in IMTA samples, with REF samples displaying a lower content of lipids in June as compared to earlier months (Fig. 6B). Protein contents (ranging from 10.51 ± 0.14% in IMTA samples from April to 8.86 ± 1.06% in IMTA samples from June) are not statistically different between IMTA and REF remaining mostly unchanged along harvesting periods (Fig. 6C).

3.4. Fatty acid composition

Twenty-one different FA were recorded in the *S. latissima* samples (Table I). Some minor FA were not detected in some samples, namely C16:2 *n*-4 and C16:4 *n*-1, only detectable in June, 20:4 *n*-3 not detected in May IMTA samples, and 22:6 *n*-3 not detected in April and May IMTA
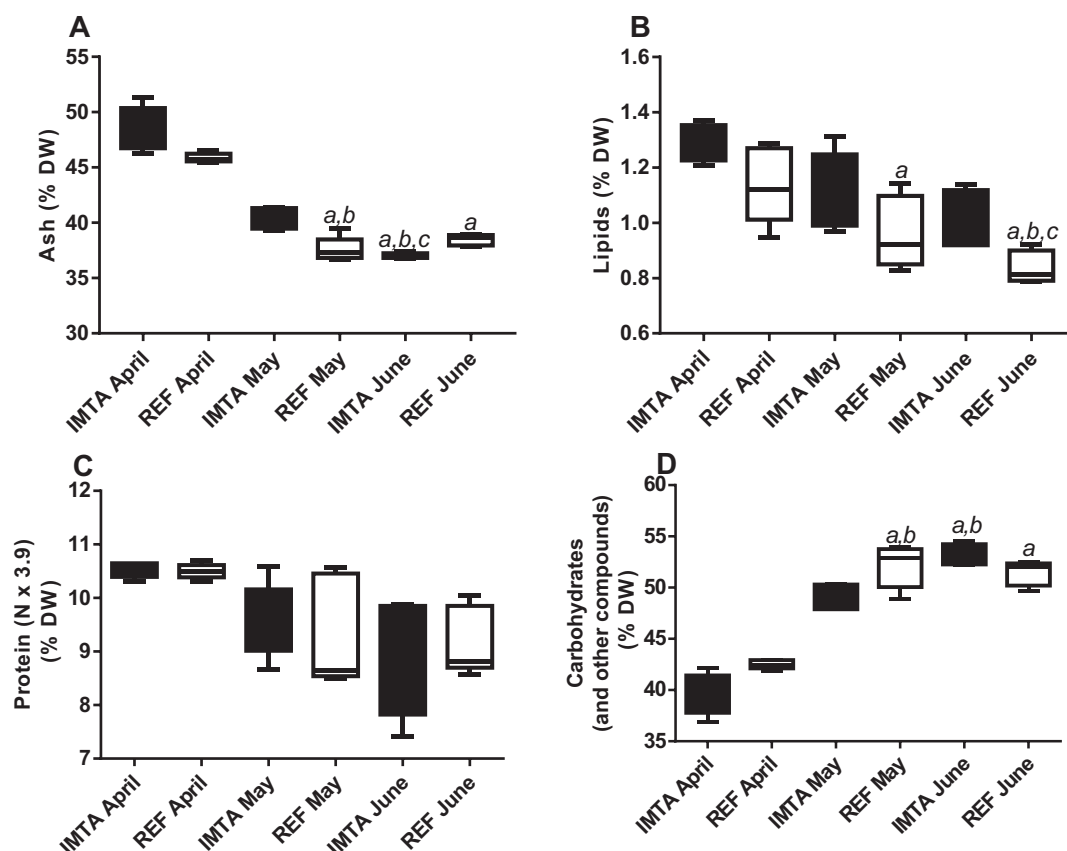
Fig. 6. Biochemical compositional analysis of *S. latissima* samples from different sites (REF or IMTA), harvested in different months (April, May and July). Content of ash (A), lipids (B) protein (C) and carbohydrates and other compounds (D) are presented as percentages of DW. IMTA: integrated multi-trophic aquaculture site; REF: reference site. Values depicted represent means ± STD for 5 replicates. Statistical significant differences ($q < 0.05$) are presented as follows: *a*: vs. IMTA April; *b*: vs. REF April; *c*: vs. IMTA May.

samples (Table I). Some FA showed variation in concentration between groups, depending mostly on harvesting period rather than on the production site. In fact, while we found many significant statistical variations when comparing different harvesting months, only 2 significantly different results from different sample sites (IMTA vs REF) in the same month were observed (for 20:4 *n*-6 in May, and for 22:6 *n*-3 in April, Table I). The most abundant FA were palmitic (16:0), oleic (18:1 *n*-9), eicosapentaenoic (20:5 *n*-3) and stearidonic (18:4 *n*-3) acids. These FA showed interchangeable position between groups in terms of abundance. Other FA were increased with harvesting time, namely C14:0 and C16:1 *n*-7, while others decreased along harvesting period, such as C18:3 *n*-3 and C18:4 *n*-3, Other FA presented a more dynamic response, increasing in the middle May month and then decreasing (in the case of C18:1 *n*-9), or decreasing from April to May and then increasing again towards June (C20:5 *n*-3). The samples with higher content in eicosapentaenoic acid (EPA, 20:5 *n*-3) and total content and *n*-3 FA were harvested in April (both IMTA and REF), and with those with the lower content were harvested in May. Therefore, harvesting month was a more impacting factor than cultivation conditions in the FA composition of *S. latissima*. Conversely, there was a statistically significant decrease in PUFA taking place between April and May in IMTA samples. A decrease in the concentration of *n*-3 FA, with a concomitant increase in *n*-6/*n*-3 ratio, was also recorded between the months of April and May for both cultivation sites, but there was an increase in June. There was a trend towards the increase in MUFA along the harvesting period (Table I).

Regarding the calculated lipid indexes (Table I), there was an increase in the saturated-to-unsaturated (SFA/UFA) ratio and a decrease in the double bond index from April to May, maintained in June. Similarly as reported for FA profile, differences in these calculated

parameters/indexes were mainly promoted by harvesting period.

3.5. Polar lipidome adaption

By analyzing the polar lipidome of *S. latissima* it was possible to detect and quantify a total of 226 lipids species (corresponding to ions with different mass-to-charge ratio - *m/z* - values) which were distributed over three main groups of polar lipids: glycolipids (55 galactolipids and 37 sulpholipids), phospholipids (125) and betaine lipids (9 DGTS) (Fig. 7). Regarding galactolipids, it was possible to identify 17 DGDG, 5 DGMG, 22 MGDG and 11 MGMG species, while in the case of sulpholipids 35 SQDG and 2 SQMG were detected. In the case of phospholipids, the lipid species identified were as following: PC (38), LPC (14), PE (21), LPE (8), PG (18), LPG (4), PI (18) and LPI (4). Results are in line with our previous works regarding *S. latissima* lipidome in samples from the same origin [15,18]. A complete list of the chemical formulae of the lipids found is shown in the supplementary data (Supplementary Table SI).

Principal component analysis (PCA) of the semi-quantification of the 226 lipid species identified originated a two-dimensional score plot representing 68.6% of the total variance, including principal component 1 (46.8%) and principal component 2 (21.8%) (Fig. 8). This plot shows a clear discrimination between samples according to harvesting period, while discrimination between cultivation sites (IMTA versus REF) is only perceptible in June.

A two-dimensional hierarchical clustering heat map presenting the top 25 most significantly discriminant polar lipid species after Kruskal-Wallis statistical analysis is presented in Fig. 9. The lipid species that contributed the most for the perceived discrimination between groups included 5 DGTS, 4 PC, 3 SQDG, 3 LPE, 3 LPC, 2 MGDG, 2 MGMG, 2

Table I

Saccharina latissima fatty acid profile (%) of samples from different types (reference (REF) or IMTA) and along three different harvesting months, and derived nutritionally and functionally-relevant parameters from fatty acid profiles.

	Mean ± STD					
	IMTA April (a)	REF April (b)	IMTA May (c)	REF May (d)	IMTA June (e)	REF June (f)
14:0	5.43 ± 0.48	6.84 ± 0.41	6.78 ± 0.31	7.70 ± 0.28	8.44 ± 0.44[a,c]	8.17 ± 0.21[a]
15:0	0.29 ± 0.18	0.23 ± 0.06	0.06 ± 0.06	0.13 ± 0.08	0.37 ± 0.04	0.34 ± 0.02
16:0	18.42 ± 0.29	17.79 ± 0.67	21.63 ± 0.54[b]	19.62 ± 0.29	18.45 ± 0.87[c]	17.97 ± 0.45[c]
16:1 n-7	0.70 ± 0.08	0.82 ± 0.02	2.61 ± 0.11[a]	1.76 ± 0.17	6.85 ± 0.18[a,b,d]	4.07 ± 0.14[a,b]
16:1	0.35 ± 0.05	0.70 ± 0.05	0.06 ± 0.06[b]	0.18 ± 0.08[b]	0.17 ± 0.11[b]	0.30 ± 0.02
16:2 n-4	0.00 ± 0.00	0.00 ± 0.00	0.00 ± 0.00	0.00 ± 0.00	0.31 ± 0.13[a,b,c,d]	0.16 ± 0.08
16:3 n-6	0.72 ± 0.10	0.90 ± 0.10	0.22 ± 0.17[b]	0.54 ± 0.06	0.36 ± 0.10[b]	0.53 ± 0.03
16:4 n-1	0.00 ± 0.00	0.00 ± 0.00	0.00 ± 0.00	0.00 ± 0.00	0.90 ± 0.07[a,b,c,d]	0.67 ± 0.58
18:0	8.11 ± 0.66	7.14 ± 0.57	10.88 ± 0.63	7.63 ± 0.38	7.66 ± 0.66	6.44 ± 0.37[c]
18:1 n-9	14.34 ± 0.26	12.94 ± 0.35	16.27 ± 0.12[b]	15.67 ± 0.14[b]	12.19 ± 0.67[c,d]	13.92 ± 0.08[c]
18:1 n-6	0.02 ± 0.02	0.00 ± 0.00	0.11 ± 0.11	0.11 ± 0.07	0.50 ± 0.14[b]	0.29 ± 0.12
18:2 n-6	7.48 ± 0.14	7.53 ± 0.15	9.76 ± 0.21[a,b]	9.15 ± 0.30[a,b]	8.68 ± 0.27	9.61 ± 0.35[a,b]
18:3 n-6	0.15 ± 0.10	0.47 ± 0.03	0.11 ± 0.11	0.72 ± 0.05	0.92 ± 0.05[a,b,c]	0.94 ± 0.05[a,b,c]
18:3 n-3	6.40 ± 0.14	6.88 ± 0.18	5.14 ± 0.17[b]	5.21 ± 0.08[b]	4.61 ± 0.27[a,b]	4.89 ± 0.16[a,b]
18:4 n-3	12.79 ± 0.24	13.71 ± 0.35	9.27 ± 0.41[a,b]	9.77 ± 0.24[b]	8.98 ± 0.26[a,b]	9.27 ± 0.20[a,b]
20:0	0.92 ± 0.13	0.48 ± 0.15	0.11 ± 0.11[a]	0.26 ± 0.16	0.39 ± 0.17	0.69 ± 0.10
20:3 n-6	0.03 ± 0.03	0.11 ± 0.07	0.00 ± 0.00	0.13 ± 0.08	0.00 ± 0.00	0.15 ± 0.09
20:4 n-6	9.63 ± 0.20	9.23 ± 0.33	8.61 ± 0.44	11.55 ± 0.20[c]	7.26 ± 0.34[a,d]	9.27 ± 0.33
20:4 n-3	0.04 ± 0.04	0.39 ± 0.10	0.00 ± 0.00	0.06 ± 0.06	0.10 ± 0.10	0.31 ± 0.13
20:5 n-3	14.19 ± 0.37	13.53 ± 0.60	8.36 ± 0.37[a,b]	9.69 ± 0.19[a,b]	12.78 ± 0.49[c]	11.99 ± 0.65
22:6 n-3	0.00 ± 0.00	0.30 ± 0.09[a]	0.00 ± 0.00	0.12 ± 0.08[b]	0.07 ± 0.07	0.03 ± 0.03
Parameters/Indexes calculated from fatty acids						
SFA	33.17 ± 0.52	32.48 ± 1.18	39.47 ± 1.36[a,b]	35.33 ± 0.40	35.33 ± 1.59	33.60 ± 0.58[c]
MUFA	15.41 ± 0.27	14.46 ± 0.39	19.05 ± 0.24[a,b]	17.72 ± 0.36	19.70 ± 0.63[a,b]	18.58 ± 0.22[b]
PUFA	51.42 ± 0.39	53.06 ± 1.48	41.49 ± 1.46[a,b]	46.94 ± 0.54	44.97 ± 1.30[a,b]	47.82 ± 0.69
n-3	33.41 ± 0.33	34.82 ± 0.99	22.77 ± 0.94[a,b]	24.85 ± 0.32[a,b]	26.54 ± 1.04	26.49 ± 0.84
n-6	18.02 ± 0.11	18.24 ± 0.51	18.82 ± 0.52	22.21 ± 0.26[a,b]	17.72 ± 0.42[d]	20.79 ± 0.58[a,e]
n-6/n-3	0.54 ± 0.01	0.52 ± 0.01	0.83 ± 0.02[a,b]	0.89 ± 0.01[a,b]	0.67 ± 0.03	0.79 ± 0.04[b]
SFA/UFA	0.50 ± 0.01	0.48 ± 0.03	0.65 ± 0.04[a,b]	0.55 ± 0.01	0.55 ± 0.04	0.51 ± 0.01[c]
ACL	17.87 ± 0.03	17.80 ± 0.04	17.58 ± 0.03[a,b]	17.68 ± 0.01	17.52 ± 0.04[a,b]	17.64 ± 0.01[a]
DBI	213.0 ± 2.1	217.4 ± 5.7	168.4 ± 5.7[a,b]	190.5 ± 1.8[b]	188.6 ± 5.2[a,b]	195.9 ± 3.5
PI	197.4 ± 2.6	201.6 ± 6.2	142.9 ± 5.9[a,b]	167.4 ± 2.0[a,b]	167.4 ± 5.1[b]	173.6 ± 4.4

IMTA: integrated multi-trophic aquaculture site; REF: reference site; SEM: standard error of mean. Values presented are means ± STD for 5 replicates (5 different production ropes). Statistical significant differences ($q < 0.05$) are presented as follows: *a*: vs. IMTA April; *b*: vs. REF April; *c*: vs. IMTA May; *d*: vs. REF May; *e*: vs. IMTA June. SFA: saturated fatty acid; MUFA: monounsaturated fatty acid; PUFA: polyunsaturated fatty acid; *n*-3: omega-3 fatty acids; *n*-6: omega-6 fatty acids; SFA/UFA: saturated to unsaturated ratio; ACL: average chain length; DBI: double bond index; PI: peroxidizability index.
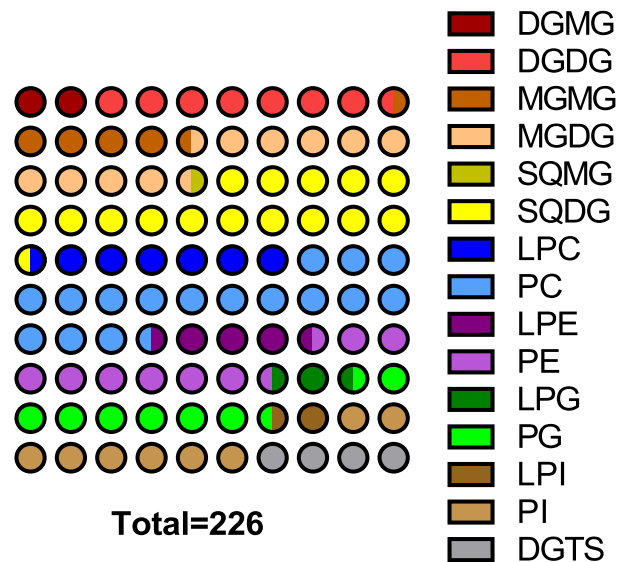

Fig. 7. Species detected by lipid class as a percentage of the total number of species detected (226). DGMG: digalactosyl-monoacylglycerol; DGDG: *diga-lactosyl*-diacylglycerol; MGMG: *monogalactosyl*-monoacylglycerol; MGDG: *monogalactosyl*-diacylglycerol; SQMG: sulfoquinovosyl-monoacylglycerol; SQDG: sulfoquinovosyl-diacylglycerol; LPC: lysophosphatidylcholine; PC: phosphatidylcholine; LPE: lysophosphatidylethanolamine; PE: phosphatidyl-ethanolamine; LPG: lysophosphatidylglycerol; PG: phosphatidylglycerol; LPI: lysophosphatidylinositol; PI: phosphatidylinositol; DGTS: diacylglyceryltrimethylhomoserine.
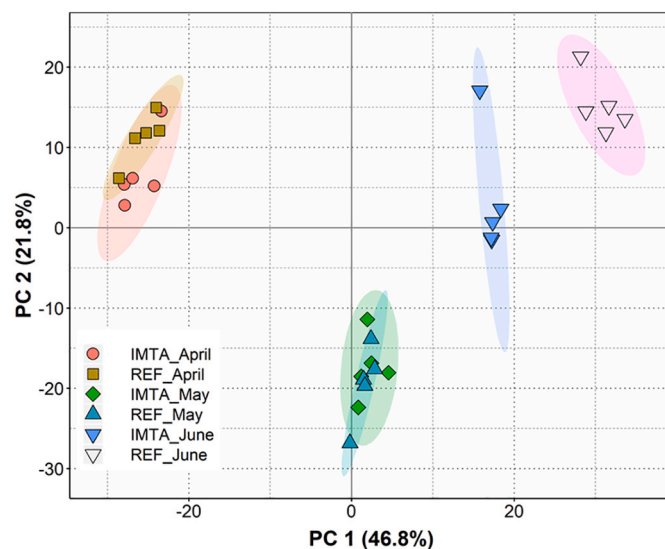

Fig. 8. Sample group discrimination with regard to polar lipid molecular content. Principal component analysis (PCA) score plot of the lipid profiles in terms of the molecular polar lipid species present in samples of *S. latissima* from different cultivation sites (integrated multi-trophic aquaculture - IMTA, or reference - REF) and collected in different months (April, May and June). Five replicates (5 different production ropes) per group were used. Royston's test indicated that, at the 0.05 significance level, the dataset follows multivariate normality.
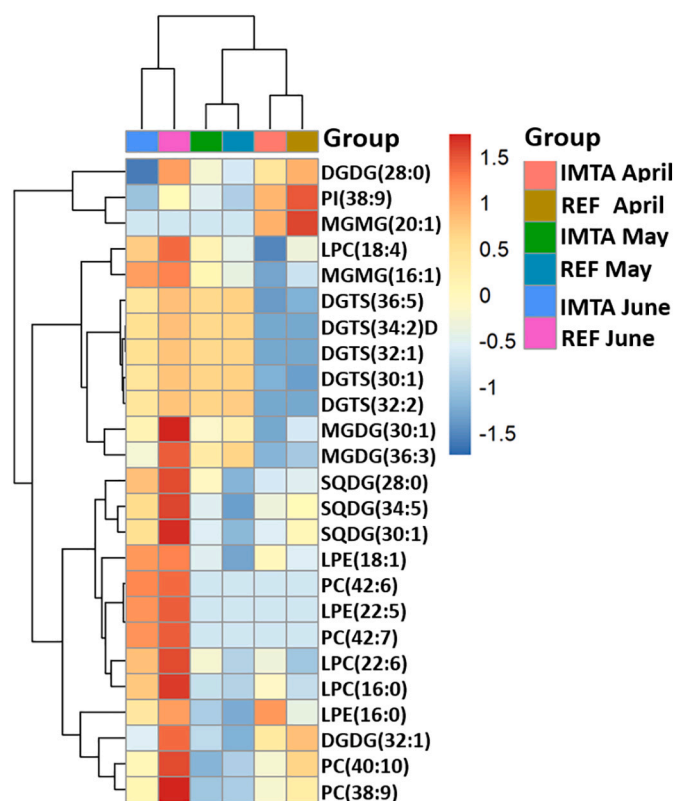
Fig. 9. Two-dimensional hierarchical clustering heat map with the 25 most significant polar lipid discriminant species after Kruskal-Wallis statistical analysis. Levels of relative abundance are shown on the color scale, with numbers indicating the fold difference from the mean. Five replicates (5 different production ropes) per group were used. Labels of the species are according to the notation AAAA (xx:i) (AAAA = lipid class; xx = total of carbon atoms in fatty acid; i = number of unsaturations). IMTA: integrated multitrophic aquaculture site; REF: reference site.

DGDG, and 1 PI, that can be grouped as 5 betaines, 11 phospholipids and 9 glycolipids. The most important differences between harvest time groups concerns betaine lipids. In April, only one DGTS species was detected, while in latter months there were a total of 9 different species found (Supplementary Table S1). As for the more significantly different PC species, they were typically highly unsaturated species (PC(42:6), PC(42:7), PC(40:10) and PC(38:9)) which are more abundant in June and less abundant in May. Lysophospholipids (LPC and LPE) were also consistently abundant in June, mostly in REF samples (some of them 8 fold higher than IMTA), and contributed to the discrimination between IMTA and REF in June. Some SQDG species presented a lower content in May than in April, with higher levels being recorded in June.

The heat map in Fig. 9 displayed a first dimension separation of the samples in three groups, according to the harvesting period. In the second dimension the samples were separated in three major groups. One group included 3 species, the DGDG(28:0), PI(38:9) and MGMG(20:1) with a higher relative abundance in April in both IMTA and REF samples. A second group included 5 betaine lipids with higher abundance in May and June, and also one LPC and one MGMG and 2 MGDG with higher abundance in June. A third group included several PC, GL, and lysoPL lipid species with higher abundance in June. This group included 4 highly unsaturated PC species, PC(42:6), PC(42:7), PC(40:10) and PC(38:9), typically more abundant in June and less abundant in May. Also, SQDG species presented lower content in May than in April, with higher contents in June. A number of lysophospholipids (LPC and LPE) were consistently in higher abundance in June, especially in samples from REF sites, which could contribute to the discrimination between farming types in June, depicted in Fig. 8.

Several differences in lipid class content (Fig. 10) were observed with harvesting period. The main differences were a higher content of DGTS in May and June as compared to April, and a higher content of LPC and LPE in June as compared to April and May. In terms of differences between cultivation sites within the same harvesting period, the main differences were recorded in June, where a higher content in phospholipid classes PC (>3 fold increase), PE (>1.6 fold increase), PG (>4 fold increase) and PI (>4 fold increase), galactolipid classes DGDG (>4 fold increase) and MGDG (>4 fold increase) and sulpholipid class SQDG (>3 fold increase) was observed in REF samples as compared to IMTA sites.

4. Discussion

The production of kelp coupled with salmon sea cage farming under an IMTA framework proved to be more efficient in terms of biomass yield. The yield-boosting effect described here confirmed what is already described for other macroalgae, and for *S. latissima* in particular [5,54]. This corresponds well with the higher simulated nutrient concentration at the IMTA than at the reference station. Our model predicts that ammonium concentrations were comparable with previous simulation studies and field data [36], despite the fact that the total salmon biomass and feed use during the period were high (Fig. 2). The reason for this is probably that the feed was distributed over a relatively high number of cages and that the water current speeds in the farm area are high [39]. The ocean model has been shown to realistically reproduce the current speed and directions at the site [39], as well as nutrient concentrations in other settings [36].

The impact of IMTA cultivation in kelp composition was never addressed before through an integrated lipidomics approach. With this approach we aimed to determine if the increase in biomass yield could have a negative impact in the nutritional value of macroalgae biomass. Anyway, other authors reported inorganic nutrient release from fish cages at IMTA sites (namely that of nitrogen/NH_4^+) to be negligible when compared to its naturally occurring amounts [55]. In our work, the average values of NO_3^- were 10 times higher than average NH_4+. However, the site is heavily influenced by tides [39] and, in May, the NO_3^- concentrations are a lot lower, and at times the NH_4+ concentrations are up to 1/3 or 1/2 of these. Nevertheless, results gathered in this study showed no significant differences in protein content between samples from IMTA and REF, despite reports stating that IMTA cultivated macroalgae display increased tissue nitrogen and protein when compared to macroalgae cultivated in reference locations [56,57] due to higher ambient nitrogen concentrations.

The observed differences in elemental and biochemical composition were mostly related to different harvesting period, with samples from April presenting lower values of carbon and hydrogen, concomitant with lower values of carbohydrates (Figs. 6 and 5). It was also possible to note a tendency for a decrease in lipid and ash content along the harvesting period (Fig. 6). The negative correlation between ash content and carbohydrate content was already documented in previous studies [11,12]. Abiotic factors such has salinity and nitrogen availability have been reported to impact carbohydrate content in *S. latissima* [58], although in this case, proximity to the salmon cages did not seem to have an effect. Moreover, carbohydrate content seemed to undergo significant seasonal variations, an effect well documented in literature (as early as 1950 [30]), and that we corroborated here in the study of samples collected in consecutive months [2].

Saccharina latissima has a modest content of lipids, and our results are also generally in accordance with what has been previously reported for this macroalgae [15,18,59,60]. Lipid content in *S. latissima* was shown to be influenced seasonally [14]. A previous study reported the lowest lipid content in July for both IMTA and REF locations [14] and the present study confirmed this trend within the period surveyed. In contrast to previous studies [14], this study allowed to pinpoint differencesbetween samples form IMTA and REF sites regarding the lipid content (DW), with REF samples displaying a tendency towards lower
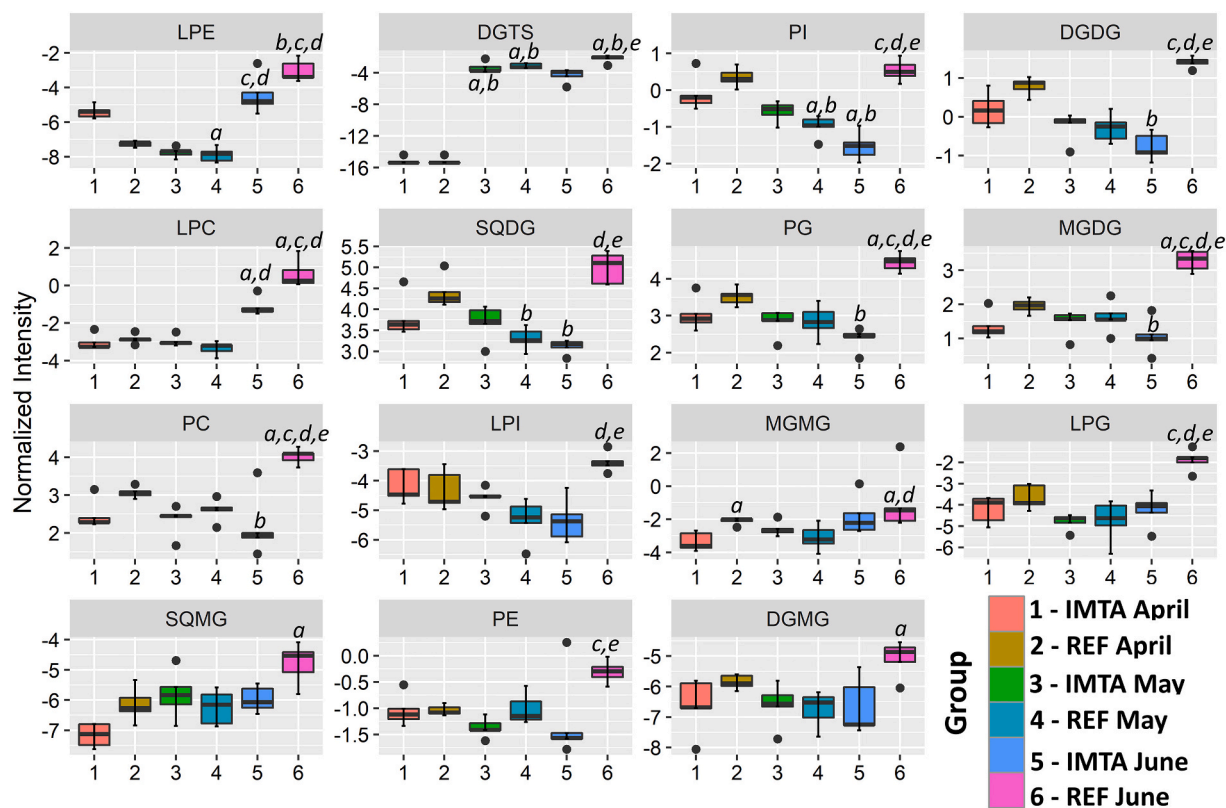
Fig. 10. Boxplot of Kruskal-Wallis significant variables depicting the lipid classes present in *S. latissima* samples from different cultivation/production sites and harvesting times, ranging from major to less discriminant. Statistical significant differences ($q < 0.05$) are presented as follows: *a*: vs. IMTA April; *b*: vs. REF April; *c*: vs. IMTA May; *d*: vs. REF May; *e*: vs. IMTA June. IMTA: integrated multi-trophic aquaculture site; REF: reference site. Five replicates (5 different production ropes) per group were used. DGMG: digalactosyl-monoacylglycerol; DGDG: *digalactosyl*-diacylglycerol; MGMG: *monogalactosyl*-monoacylglycerol; MGDG: *monogalactosyl*-diacylglycerol; SQMG: sulfoquinovosyl-monoacylglycerol; SQDG: sulfoquinovosyl-diacylglycerol; LPC: lysophosphatidylcholine; PC: phosphatidylcholine; LPE: lysophosphatidylethanolamine; PE: phosphatidylethanolamine; LPG: lysophosphatidylglycerol; PG: phosphatidylglycerol; LPI: lysophosphatidylinositol; PI: phosphatidylinositol; DGTS: diacylglyceryltrimethylhomoserine.

content, especially in June (comparing with IMTA samples from previous months).

Saccharina latissima FA profile was analyzed by GC–MS and is generally in agreement with what has been described in previous studies [15,18]. The analysis of the FA profile confirms that harvesting period is a strong factor modulating kelp composition, more relevant than the proximity to fish sea cages in IMTA setups (Table I). Almost all significant statistical differences (with the exception of only two) were related to harvesting period, rather than with of sample type (IMTA or REF). In fact, a previous study did not report any major changes between lipid and FA contents between *S. latissima* IMTA and REF samples [14], in line with the results gathered herein. Therefore, conditions related to harvesting time, probably associated with variations in local abiotic conditions, have a more marked effect on FA content. In that sense, the observed increase in the SFA/UFA ratio and the decrease in the DBI from April to May could be related with alteration of abiotic conditions, although our observations point to a marginal temperature increase throughout those months ($\approx$2 °C in a nearby location [35]). Nevertheless, the decrease of FA unsaturation in the warmer months was already reported for this kelp [16,33]. Temperature has been suggested to be a decisive factor for the chemical composition of *S. latissima* [11], while light intensity, although reported as impacting FA content in macroalgae, appears to drive less consistent effects [61–65].

Between April and May there is a noticeable decrease in *n*-3 FA, and therefore an increase in the *n*-6/*n*-3 ratio for both IMTA and REF samples. This should be taken into consideration when choosing the harvesting time and the ultimate targets of production, as the content in *n*-3 FA substantiates some of the appeal of macroalgae as food products, and

increases their attractiveness as potential functional foods. A previous study reported an increase in C20:5 *n*-3 with a concomitant decrease in the *n*-6/*n*-3 ratio, in samples from IMTA when compared to biomass harvested in the wild, a trend that we did not observe in this study when comparing our samples from IMTA with REF locations [16].

Regarding the polar lipidome analysis, results are in line with our previous works regarding *S. latissima* lipidome in samples from the same origin [15,18]. The harvesting period seems to be an important modulation factor, as seen by the discrimination between harvesting periods, but not between farming conditions, as denoted in the PCA plot (Fig. 8). As major contributors to those differences, we have some DGTS and PC species, but also some lysophospholipids (namely LPC an LPE) (Fig. 9). DGTS and PC are polar lipids that are the main components of the cell membranes of macroalgae, performing similar functions particularly in non-thylakoid membranes [66]. In fact, they share a similar zwitterionic structure and, more interestingly, their contents were found to be interchangeable, with DGTS being proposed as substitutes for PC in phosphorus-depleted environments [67,68]. Variation in betaine lipid profile has been related to temperature adaptation processes in microalgae [66,69,70] *and plants* [71]*, and therefore the observed increase in some DGTS species may typify an acclimation process (water temperature in the area increased from* $\approx$5 °C to $\approx$10 °C *during the timespan of the study* [35]). Also, the relative content of lyso phospholipids, namely LPC and LPE (Figs. 9 and 10) was remarkably higher in June samples. Lysophospholipids are recognized as important components of cell membranes, but also play important physiological roles as second-messengers [72]. The increase in these lysophospholipids (LPC, LPE) was reported in wounded plants [73], as well as in temperature

acclimation processes [74]. Therefore, the observed higher abundance of some lysophospholipids in June may be related to acclimation to different sea conditions and may reflect a degree of plasticity towards more extreme summer circumstances. However, a synergetic effect between several environmental stressors or factors should not be discarded as impacting the lipid composition of *S. latissima*. Biofouling might be one of those stressors. However, biofouling on the kelp lamina typically occurs from June onwards in the experimental area, with filamentous algae dominating early in the season while the bryozoans (*Membranipora membranacea*) strongly dominate from July until loss of biomass in August/September [40]. The biomass used for chemical analysis was harvested before severe biofouling settlement and thus it should have a negligible influence on the results.

A very interesting result is the discrimination between cultivation sites (IMTA vs REF) in June. Several lipid classes are increased in REF samples regarding IMTA counterparts, including lysophospholipids (LPI, LPG), phospholipids (PI, PG, PC, PE), betaine lipids, glycolipids (DGDG, MGDG), and sulpholipids (SQDG) (Fig. 10). It is interesting that lysophospholipids, in this case specifically LPI and LPG species (and not LPC and LPE, which contributed more to the discrimination between June and the previous months), are the ones increased in REF samples from June. The accumulation of lysophospholipids in plants is known to occur under many different stress situations (freezing, wounding, pathogen infection or the application of elicitors [73,75–78], and it would be interest to consider if different stressors elicit the accumulation of different lysophospholipids. Nevertheless, differences in lysophospholipids according to production site in *S. latissima* were already reported corroborating the results from the present study [18]). Therefore the potential of these species for traceability or as biomarkers of environmental stress should be further studied in the future, especially in a context of global climatic change. In fact, these lipid species could also represent new tools for kelp production practices, as possible indicative markers for the evaluation of the adaptation of local ecotypes for cultivation in different areas.

5. Conclusion

In this study we explored time of harvesting and the proximity to fish sea cages in IMTA facilities as factors impacting *S. latissima* composition and nutritional quality. Harvesting period had clearly more impact on *S. latissima* composition than cultivation site (IMTA or REF). IMTA macroalgae production represents a consolidated manner of producing kelp biomass with similar quality as REF sites, with the advantages of generating greater biomass yields, and mitigating the environmental toll of intensive fish aquaculture. Moreover, when aiming at the exploitation of lipid compounds of interest or lipid-related beneficial effects, IMTA production should be prioritized since it guarantees more lipid yield per area, while displaying similar quality. This study also represents a step forward in order to pinpoint the stability the composition of farmed biomass. Ultimately, these findings should be thoroughly considered when targeting certain compounds of interest and will inestimably contribute to boost the sustainable production of macroalgae in IMTA setups.

Author contributions statement

João P. Monteiro: Conceptualization, Methodology, Investigation, Data Curation, Writing - Original Draft **Tânia Melo:** Investigation, Writing - Review & Editing **Jorunn Skjermo:** Conceptualization, Resources, Writing - Review & Editing **Silje Forbord:** Investigation, Resources, Writing - Review & Editing **Ole J. Broch:** Conceptualization, Methodology, Formal analysis **Pedro Domingues:** Formal analysis, Writing - Review & Editing **Ricardo Calado:** Writing - Review & Editing **M. Rosário Domingues:** Conceptualization, Methodology, Writing - Review & Editing.

Declaration of competing interest

The authors declare that they have no known competing financial interests or personal relationships that could have appeared to influence the work reported in this paper.

References

[1] P. MacArtain, C.I.R. Gill, M. Brooks, R. Campbell, I.R. Rowland, Nutritional value of edible seaweeds, Nutr. Rev. 65 (2007) 535–543.

[2] S.L. Holdt, S. Kraan, Bioactive compounds in seaweed: functional food applications and legislation, J. Appl. Phycol. 23 (2011) 543–597.

[3] S. Khalid, M. Abbas, F. Saeed, H. Bader-Ul-Ain, H.A.R. Suleria, Therapeutic potential of seaweed bioactive compounds, in: S. Maiti (Ed.), Seaweed Biomaterials, IntechOpen, London, United Kingdom, 2018.

[4] Food and Agriculture Organization of the United Nations, The State of World Fisheries and Aquaculture 2018 – Meeting the sustainable development goals (2018) 277.

[5] A. Handå, S. Forbord, X. Wang, O.J. Broch, S.W. Dahle, T.R. Størseth, K.I. Reitan, Y. Olsen, J. Skjermo, Seasonal- and depth-dependent growth of cultivated kelp (Saccharina latissima) in close proximity to salmon (Salmo salar) aquaculture in Norway, Aquaculture 414-415 (2013) 191–201.

[6] C. Peteiro, N. Sánchez, B. Martínez, Mariculture of the Asian kelp Undaria pinnatifida and the native kelp Saccharina latissima along the Atlantic coast of southern Europe: an overview, Algal Res. 15 (2016) 9–23.

[7] C. Peteiro, Ó. Freire, Biomass yield and morphological features of the seaweed Saccharina latissima cultivated at two different sites in a coastal bay in the Atlantic coast of Spain, J. Appl. Phycol. 25 (2013) 205–213.

[8] M. Olischläger, C. Iñiguez, F.J.L. Gordillo, C. Wiencke, Biochemical composition of temperate and Arctic populations of Saccharina latissima after exposure to increased pCO2 and temperature reveals ecotypic variation, Planta 240 (2014) 1213–1224.

[9] K. Ehrig, S. Alban, Sulfated galactofucan from the brown alga *Saccharina latissima*—variability of yield, structural composition and bioactivity, Mar Drugs 13 (2015) 76–101.

[10] X. Zhang, M. Thomsen, Biomolecular composition and revenue explained by interactions between extrinsic factors and endogenous rhythms of Saccharina latissima, Mar Drugs 17 (2019) 107.

[11] D.M. Manns, M.M. Nielsen, A. Bruhn, B. Saake, A.S. Meyer, Compositional variations of brown seaweeds Laminaria digitata and *Saccharina latissima* in Danish waters, J. Appl. Phycol. 29 (2017) 1493–1506.

[12] S. Sharma, L. Neves, J. Funderud, L.T. Mydland, M. Øverland, S.J. Horn, Seasonal and depth variations in the chemical composition of cultivated Saccharina latissima, Algal Res. 32 (2018) 107–112.

[13] I.C. Azevedo, P.M. Duarte, G.S. Marinho, F. Neumann, I. Sousa-Pinto, Growth of Saccharina latissima (Laminariales, Phaeophyceae) cultivated offshore under exposed conditions, Phycologia 58 (2019) 504–515.

[14] G.S. Marinho, S.L. Holdt, C. Jacobsen, I. Angelidaki, Lipids and composition of fatty acids of Saccharina latissima cultivated year-round in integrated multitrophic aquaculture, Mar Drugs 13 (2015) 4357–4374.

[15] F. Rey, D. Lopes, E. Maciel, J. Monteiro, J. Skjermo, J. Funderud, D. Raposo, P. Domingues, R. Calado, M.R. Domingues, Polar lipid profile of Saccharina latissima, a functional food from the sea, Algal Res. 39 (2019) 101473.

[16] M. Barbosa, F. Fernandes, D.M. Pereira, I.C. Azevedo, I. Sousa-Pinto, P.B. Andrade, P. Valentão, Fatty acid patterns of the kelps Saccharina latissima, Saccorhiza polyschides and Laminaria ochroleuca: influence of changing environmental conditions, Arab. J. Chem. 1 (2017) 45–58.

[17] M. Schmid, F. Guihéneuf, D.B. Stengel, Fatty acid contents and profiles of 16 macroalgae collected from the Irish coast at two seasons, J. Appl. Phycol. 26 (2014) 451–463.

[18] J.P. Monteiro, F. Rey, T. Melo, A.S.P. Moreira, J.-F. Arbona, J. Skjermo, S. Forbord, J. Funderud, D. Raposo, P.D. Kerrison, M.-M. Perrineau, C. Gachon, P. Domingues, R. Calado, M.R. Domingues, The unique lipidomic signatures of Saccharina latissima can be used to pinpoint their geographic origin, Biomolecules 10 (2020) 107.

[19] D.B. Sudatti, M.T. Fujii, S.V. Rodrigues, A. Turra, R.C. Pereira, Effects of abiotic factors on growth and chemical defenses in cultivated clones of Laurencia dendroidea J. Agardh (Ceramiales, Rhodophyta), Marine Biology 158 (2011) 1439–1446.

[20] E.A. Shalaby, Influence of abiotic stress on biosynthesis of alga-chemicals and its relation to biological activities, Indian Journal of Geo Marine Sciences 46 (2017) 23–32.

[21] Y. Ji, Z. Xu, D. Zou, K. Gao, Ecophysiological responses of marine macroalgae to climate change factors, J. Appl. Phycol. 28 (2016) 2953–2967.

[22] D.B. Stengel, S. Connan, Z.A. Popper, Algal chemodiversity and bioactivity: sources of natural variability and implications for commercial application, Biotechnol. Adv. 29 (2011) 483–501.

[23] T.M. Mata, A.A. Martins, N.S. Caetano, Microalgae for biodiesel production and other applications: a review, Renew. Sust. Energ. Rev. 14 (2010) 217–232.

[24] S.P. Singh, P. Singh, Effect of temperature and light on the growth of algae species: a review, Renew. Sust. Energ. Rev. 50 (2015) 431–444.

[25] I.-C. Chung, R.-L. Hwang, S.-H. Lin, T.-M. Wu, J.-Y. Wu, S.-W. Su, C.-S. Chen, T.-M. Lee, Nutrients, temperature, and salinity as primary factors influencing the temporal dynamics of macroalgal abundance and assemblage structure on a reef of Du-Lang Bay in Taitung in southeastern Taiwan, Bot. Stud. 48 (2007) 419–433.

[26] D. Stengel, R. Conde-Álvarez, S. Connan, U. Nitschke, F. Arenas, H. Abreu, J. B. Barufi, F. Chow, D. Robledo, E. Malta, Short-term effects of CO2, nutrients and temperature on three marine macroalgae under solar radiation, Aquat. Biol. 22 (2014) 159–176.

[27] A.S. Carlsson, D.J. Bowles, Micro- and macro-algae: utility for industrial applications: outputs from the EPOBIO project, CPL Press, Speen (September 2007) 2007.

[28] M.J. Pérez, E. Falqué, H. Domínguez, Antimicrobial action of compounds from marine seaweed, Mar Drugs 14 (2016) 52.

[29] M. Vitova, K. Bisova, S. Kawano, V. Zachleder, Accumulation of energy reserves in algae: from cell cycles to biotechnological applications, Biotechnol. Adv. 33 (2015) 1204–1218.

[30] W.A.P. Black, The seasonal variation in weight and chemical composition of the common British Laminariaceae, J. Mar. Biol. Assoc. U. K. 29 (1950) 45–72.

[31] P. Schiener, K.D. Black, M.S. Stanley, D.H. Green, The seasonal variation in the chemical composition of the kelp species Laminaria digitata, Laminaria hyperborea, Saccharina latissima and Alaria esculenta, Journal of Applied Phycology 27 (2015) 363–373.

[32] J.M.M. Adams, A.B. Ross, K. Anastasakis, E.M. Hodgson, J.A. Gallagher, J. M. Jones, I.S. Donnison, Seasonal variation in the chemical composition of the bioenergy feedstock Laminaria digitata for thermochemical conversion, Bioresour. Technol. 102 (2011) 226–234.

[33] J.V. Vilg, G.M. Nylund, T. Werner, L. Qvirist, J.J. Mayers, H. Pavia, I. Undeland, E. Albers, Seasonal and spatial variation in biochemical composition of Saccharina latissima during a potential harvesting season for Western Sweden, Bot. Mar. 58 (2015) 435.

[34] S. Forbord, K.B. Steinhovden, K.K. Rød, A. Handå, J. Skjermo, Cultivation protocol for Saccharina latissima, in: B. Charrier, O.T. Wichard, C.R.K. Reddy (Eds.), Protocols for Macroalgae Research, 1st Edn., Boca Raton, FL, US, 2018, pp. 37–59.

[35] S. Forbord, K.B. Steinhovden, T. Solvang, A. Handå, J. Skjermo, Effect of seeding methods and hatchery periods on sea cultivation of Saccharina latissima (Phaeophyceae): a Norwegian case study, J. Appl. Phycol. 32 (2020) 2201–2212.

[36] H. Jansen, O. Broch, R. Bannister, P. Cranford, A. Handå, V. Husa, Z. Jiang, T. Strohmeier, Ø. Strand, Spatio-temporal Dynamics in the Dissolved Nutrient Waste Plume from Norwegian Salmon Cage Aquaculture, Aquaculture Environment Interactions, 10, 2018.

[37] D. Slagstad, T.A. McClimans, Modeling the ecosystem dynamics of the Barents Sea including the marginal ice zone: I. physical and chemical oceanography, J. Mar. Syst. 58 (2005) 1–18.

[38] O.J. Broch, R.L. Daae, I.H. Ellingsen, R. Nepstad, E.Å. Bendiksen, J.L. Reed, G. Senneset, Spatiotemporal Dispersal and Deposition of Fish Farm Wastes: A Model Study from Central Norway, Frontiers in Marine Science, 4, 2017.

[39] O.J. Broch, P. Klebert, F.A. Michelsen, M.O. Alver, Multiscale modelling of cage effects on the transport of effluents from open aquaculture systems, PLoS One 15 (2020), e0228502.

[40] S. Forbord, S. Matsson, G.E. Brodahl, B.A. Bluhm, O.J. Broch, A. Handå, A. Metaxas, J. Skjermo, K.B. Steinhovden, Y. Olsen, Latitudinal, seasonal and depth-dependent variation in growth, chemical composition and biofouling of cultivated Saccharina latissima (Phaeophyceae) along the Norwegian coast, J. Appl. Phycol. 32 (2020) 2215–2232.

[41] E. da Costa, T. Melo, A.S.P. Moreira, C. Bernardo, L. Helguero, I. Ferreira, M. T. Cruz, A.M. Rego, P. Domingues, R. Calado, M.H. Abreu, M.R. Domingues, Valorization of lipids from Gracilaria sp. through lipidomics and decoding of antiproliferative and anti-inflammatory activity, Mar Drugs 15 (2017) 62.

[42] T. Pluskal, S. Castillo, A. Villar-Briones, M. Orešič, MZmine 2: modular framework for processing, visualizing, and analyzing mass spectrometry-based molecular profile data, BMC Bioinformatics 11 (2010) 395.

[43] R.C. Team, R Foundation for Statistical Computing; Vienna, Austria: 2018, R: A Language and Environment for Statistical Computing, (2018), 2013.

[44] R. Team, RStudio: Integrated Development Environment for R., Inc., Boston, MA vol 14, 2016.

[45] J. Xia, I.V. Sinelnikov, B. Han, D.S. Wishart, MetaboAnalyst 3.0–making metabolomics more meaningful, Nucleic Acids Res. 43 (2015) W251–W257.

[46] D. Murdoch, E.D. Chow, Ellipse: Functions for Drawing Ellipses and Ellipse-like Confidence Regions, R Package Version 0.3–8, 2018.

[47] J.P. Royston, Some techniques for assessing multivarate normality based on the Shapiro- Wilk W, J. R. Stat. Soc.: Ser. C: Appl. Stat. 32 (1983) 121–133.

[48] S. Korkmaz, D. Goksuluk, G. Zararsiz, MVN: an R package for assessing multivariate normality, The R Journal 6 (2014) 151–162.

[49] R. Kolde, Pheatmap: Pretty Heatmaps, R Package Version 1.0.12, 2019.

[50] H. Wickham, Ggplot2: Elegant Graphics for Data Analysis, Springer-Verlag, New York, 2016.

[51] H. Wickham, The Split-Apply-Combine Strategy for Data Analysis, 2011 40, 2011, p. 29.

[52] H. Wickham, R. Francois, L. Henry, K. Müller, dplyr: A Grammar of Data Manipulation. R Package Version 0.7.7, 2018.

[53] H. Wickham, L. Henry, tidyr: Easily Tidy Data With 'Spread ( )' and 'Gather ( )' Functions, R Package Version 0.8.1 vol 3, 2018.

[54] J. Fossberg, S. Forbord, O.J. Broch, A.M. Malzahn, H. Jansen, A. Handå, H. Førde, M. Bergvik, A.L. Fleddum, J. Skjermo, Y. Olsen, The Potential for Upscaling Kelp (Saccharina Latissima) Cultivation in Salmon-Driven Integrated Multi-Trophic Aquaculture (IMTA), Frontiers in Marine Science, 5, 2018.

[55] G.S. Marinho, S.L. Holdt, M.J. Birkeland, I. Angelidaki, Commercial cultivation and bioremediation potential of sugar kelp, Saccharina latissima, in Danish waters, Journal of Applied Phycology 27 (2015) 1963–1973.

[56] T. Chopin, C. Yarish, R. Wilkes, E. Belyea, S. Lu, A. Mathieson, Developing Porphyra/salmon integrated aquaculture for bioremediation and diversification of the aquaculture industry, J. Appl. Phycol. 11 (1999) 463.

[57] M.H. Abreu, D.A. Varela, L. Henríquez, A. Villarroel, C. Yarish, I. Sousa-Pinto, A. H. Buschmann, Traditional vs. integrated multi-trophic aquaculture of Gracilaria chilensis, in: C.J. Bird, J. McLachlan, E.C. Oliveira (Eds.), Productivity and Physiological Performance, Aquaculture vol. 293, 2009, pp. 211–220.

[58] M.M. Nielsen, D. Manns, M. D'Este, D. Krause-Jensen, M.B. Rasmussen, M. M. Larsen, M. Alvarado-Morales, I. Angelidaki, A. Bruhn, Variation in biochemical composition of Saccharina latissima and Laminaria digitata along an estuarine salinity gradient in inner Danish waters, Algal Res. 13 (2016) 235–245.

[59] G.S. Marinho, M. Alvarado-Morales, I. Angelidaki, Valorization of macroalga Saccharina latissima as novel feedstock for fermentation-based succinic acid production in a biorefinery approach and economic aspects, Algal Res. 16 (2016) 102–109.

[60] S.M. Tibbetts, J.E. Milley, S.P. Lall, Nutritional quality of some wild and cultivated seaweeds: nutrient composition, total phenolic content and in vitro digestibility, J. Appl. Phycol. 28 (2016) 3575–3585.

[61] E.A.T. Floreto, S. Teshima, The fatty acid composition of seaweeds exposed to different levels of light intensity and salinity, Bot. Mar. 41 (1998) 467–482.

[62] I. Levy, C. Maxim, M. Friedlander, Fatty acid distribution among some red algal macrophytes, J. Phycol. 28 (1992) 299–304.

[63] E.A.T. Floreto, H. Hirata, S. Ando, S. Yamasaki, Effects of temperature, light intensity, salinity and source of nitrogen on the growth, total lipid and fatty acid composition of Ulva pertusa Kjellman (Chlorophyta), Bot. Mar. 36 (1993) 149.

[64] C.J. Dawes, C. Kovach, M. Friedlander, Exposure of Gracilaria to various environmental conditions. II. The effect on fatty acid composition, Bot. Mar. 36 (1993) 289–296.

[65] E. Pinto, A.P. Carvalho, K.H.M. Cardozo, F.X. Malcata, F.M.D. Anjos, P. Colepicolo, Effects of heavy metals and light levels on the biosynthesis of carotenoids and fatty acids in the macroalgae Gracilaria tenuistipitata (var. liui Zhang & Xia), Revista Brasileira de Farmacognosia 21 (2011) 349–354.

[66] H. Murakami, T. Nobusawa, K. Hori, M. Shimojima, H. Ohta, Betaine lipid is crucial for adapting to low temperature and phosphate deficiency in Nannochloropsis, Plant Physiol. 177 (2018) 181–193.

[67] V.J.T.V. Ginneken, A. Gittenberger, M. Rensing, E.D. Vries, E.T.H.M. Peeters, E. Verheij, Seaweed competition: Ulva sp. has the potential to produce the betaine lipid diacylglyceryl-O-4′-(N,N,N,-trimethyl) homoserine (DGTS) in order to replace phosphatidylcholine (PC) under phosphate-limiting conditions in the P-limited dutch Wadden Sea and outcompete an aggressive non-indigenous Gracilaria vermiculophylla red drift algae out of this unique UNESCO world heritage coastal area, Oceanography and Fisheries Open Access Journal 2 (2017).

[68] F.Q.Y. Goh, J. Jeyakani, P. Tipthara, A. Cazenave-Gassiot, R. Ghosh, N. Bogard, Z. Yeo, G.K.-S. Wong, M. Melkonian, M.R. Wenk, N.D. Clarke, Gains and losses of metabolic function inferred from a phylotranscriptomic analysis of algae, Sci. Rep. 9 (2019) 10482.

[69] S. Willette, S.S. Gill, B. Dungan, T.M. Schaub, J.M. Jarvis, R.St. Hilaire, F. Omar Holguin, Alterations in lipidome and metabolome profiles of Nannochlorposis salina in response to reduced culture temperature during sinusoidal temperature and light, Algal Res. 32 (2018) 79–92.

[70] S.S. Gill, S. Willette, B. Dungan, J.M. Jarvis, T. Schaub, D.M. VanLeeuwen, R. St. Hilaire, F.O. Holguin, Suboptimal temperature acclimation affects Kennedy pathway gene expression, lipidome and metabolite profile of Nannochloropsis salina during PUFA enriched TAG synthesis, Marine Drugs 16 (2018) 425.

[71] A. Sakamoto, N. Murata, The role of glycine betaine in the protection of plants from stress: clues from transgenic plants, Plant Cell Environ. 25 (2002) 163–171.

[72] A. Grzelczyk, E. Gendaszewska-Darmach, Novel bioactive glycerol-based lysophospholipids: new data – new insight into their function, Biochimie 95 (2013) 667–679.

[73] S. Lee, S. Suh, S. Kim, R.C. Crain, J.M. Kwak, H.-G. Nam, Y. Lee, Systemic elevation of phosphatidic acid and lysophospholipid levels in wounded plants, Plant J. 12 (1997) 547–556.

[74] R. Welti, W. Li, M. Li, Y. Sang, H. Biesiada, H.-E. Zhou, C.B. Rajashekar, T. D. Williams, X. Wang, Profiling membrane lipids in plant stress responses: role of phospholipase Dalpha in freezing-induced lipid changes in Arabidopsis, J. Biol. Chem. 277 (2002) 31994–32002.

[75] G.F. Scherer, Secondary messengers and phospholipase A2 in auxin signal transduction, Plant Mol. Biol. 49 (2002) 357–372.

[76] K. Viehweger, B. Dordschbal, W. Roos, Elicitor-activated phospholipase a(2) generates lysophosphatidylcholines that mobilize the vacuolar H(+) pool for pH signaling via the activation of Na(+)-dependent proton fluxes, Plant Cell 14 (2002) 1509–1525.

[77] R. Welti, W. Li, M. Li, Y. Sang, H. Biesiada, H.E. Zhou, C.B. Rajashekar, T. D. Williams, X. Wang, Profiling membrane lipids in plant stress responses. Role of phospholipase D alpha in freezing-induced lipid changes in Arabidopsis, J. Biol. Chem. 277 (2002) 31994–32002.

[78] S.J. Wi, S. Seo, K. Cho, M.H. Nam, K.Y. Park, Lysophosphatidylcholine enhances susceptibility in signaling pathway against pathogen infection through biphasic production of reactive oxygen species and ethylene in tobacco plants, Phytochemistry 104 (2014) 48–59.